

Highlights

Deep learning for chemical kinetic modeling in ammonia-methane combustion with a posteriori validation

Ke Xiao, Yangchen Xu, Han Li, Zhi X. Chen

- DNN models replace direct integration of NH₃/CH₄ chemical kinetics.
- Data augmentation based on flame structure physics improves training data quality.
- DNNs demonstrate strong predictive accuracy in unseen flame scenarios.
- Up to 20× acceleration in combustion modeling is achieved.

Deep learning for chemical kinetic modeling in ammonia-methane combustion with a posteriori validation

Ke Xiao^{a,b}, Yangchen Xu^{a,b}, Han Li^{a,b,*}, Zhi X. Chen^{a,b}

^a*State Key Laboratory of Turbulence and Complex Systems, College of Engineering,
Peking University, Beijing 100871, China*

^b*AI for Science Institute (AISI), Beijing 100080, China*

Abstract

Deep learning has shown considerable potential for alleviating the primary computational bottleneck in combustion simulations: the direct integration of stiff chemical ordinary differential equations (ODEs) in chemical kinetic modeling. This study investigates the application of deep neural networks (DNNs) as surrogate models for chemical kinetics in ammonia–methane combustion. Thermochemical training data are generated through manifold sampling of one-dimensional (1D) freely propagating premixed laminar flames. To address data imbalance near the flame front, where steep temperature gradients are present, a hybrid interpolation and randomization-based data augmentation strategy is introduced to enrich underrepresented regions in the training dataset. This refinement enhances model accuracy in 1D laminar flame validation tests. Furthermore, *a posteriori* evaluation in a two-dimensional (2D) propagating flame under homogeneous isotropic turbulence

*Corresponding author

Email address: han_li@pku.edu.cn (Han Li)

(HIT) demonstrates that the trained DNN models retain predictive accuracy under previously unseen conditions while achieving up to a $20\times$ overall speedup in computational performance. These results highlight the potential of DNN-based chemical kinetics to accelerate ammonia combustion modeling, supporting more efficient and scalable high-fidelity simulations for practical applications.

Keywords: Deep learning, Chemical kinetics, Ammonia-methane blends, Combustion modeling

1. Introduction

Ammonia has gained significant attention as a carbon-free fuel and hydrogen carrier [1, 2, 3, 4], aligning with the United Nations' Sustainable Development Goals (SDGs), which aim to pursue sustainable energy solutions that are accessible, reliable, and environmentally friendly. Key benefits of ammonia as a fuel include its zero carbon content, high volumetric energy density, and an established infrastructure for production, storage, and transport [5, 6]. However, challenges such as low flammability, low radiation intensity, and high NO_x emissions due to its nitrogen content necessitate further research to enhance ammonia combustion. Significant efforts have focused on blending ammonia with highly reactive fuels, such as hydrogen, methane, syngas, and dimethyl ether, to improve overall combustion properties like burning velocity and adiabatic flame temperature, thus enabling the use of ammonia in existing combustion systems with minimal modifications [7].

Numerical simulations are crucial for understanding the complex interac-

tions in ammonia-based fuel blends and optimizing their combustion characteristics. To achieve this, detailed finite-rate chemistry models are essential, as they provide more fundamental insights into combustion phenomena, particularly for ammonia-fueled systems, where flame instability dynamics can be pronounced [8]. However, incorporating detailed chemical kinetics significantly increases computational costs, especially in simulations involving ammonia blends, where comprehensive chemical mechanisms typically consist of dozens of species [9]. Description of chemistry using these mechanisms requires direct integration of stiff systems of ordinary differential equations (ODEs) that govern species concentration evolution. The stiffness, stemming from the wide range of chemical timescales, necessitates extremely small time steps for stable and accurate integration, thereby making the process highly computationally demanding. In practical simulations, chemistry evaluation alone can account for over 90% of total computational time, posing a major bottleneck in high-fidelity combustion modeling.

Recently, machine learning techniques for accelerating chemistry-related computations have gained increasing interest [10, 11, 12, 13]. Deep learning, a subset of machine learning utilizing deep neural networks (DNNs) to model complex patterns in large datasets, has been applied in combustion simulations as an alternative to traditional ODE integrators. By framing the integration process as a regression problem—predicting changes in species concentrations over time based on initial conditions—deep learning models can approximate chemical source terms without the need for stiff ODE integration at each time step. This approach can also be viewed as a form of data storage and retrieval or tabulation, as DNNs learn patterns from extensive

42 datasets of precomputed chemistry calculations and perform inference with
43 new, unseen data during simulations [14, 15].

44 Compared to traditional tabulation methods, DNNs avoid the need for
45 dimension reduction, which can compromise accuracy. They typically require
46 significantly less memory [16], since they only need to store a set of model
47 parameters and weights instead of input-output pairs. Furthermore, DNN in-
48 ference benefits from modern Graphics Processing Units (GPUs), optimized
49 for parallel computation, which enables rapid processing of multiple inputs
50 simultaneously. This greatly enhances inference speed and makes real-time
51 evaluations feasible in complex chemical systems. However, challenges such
52 as data curation, model selection, evaluation, and validation remain signifi-
53 cant hurdles, limiting the broader application of this methodology.

54 Addressing these hurdles begins with the creation of high-quality training
55 datasets, since the effectiveness and reliability of DNN-based chemistry mod-
56 els directly depend on the representativeness of their data. Due to the limited
57 extrapolation capabilities of data-driven methods, researchers have focused
58 on constructing datasets that encompass thermochemical states representa-
59 tive of those encountered in later combustion simulations. For instance, An
60 et al. [17] sampled data from a Reynolds-Averaged Navier-Stokes (RANS)
61 pre-simulation and applied their models in Large Eddy Simulations (LES) of
62 the same problem, while Chi et al. [18] utilized on-the-fly training in Direct
63 Numerical Simulations (DNS) to ensure that the training data is representa-
64 tive of inference data.

65 While problem-specific sampling from the target case ensures high fidelity,
66 it often limits the generalizability and reusability of DNN-based chemistry

models across diverse scenarios. To address this, researchers have adopted generic canonical problem sampling, leveraging fundamental reacting-flow configurations to generate broadly representative thermochemical datasets. For example, Wan et al. [19] sampled data from turbulent, non-adiabatic, non-premixed micro-mixing canonical problems and applied the trained neural networks to DNS of a syngas turbulent oxy-flame. Similar configurations were also used by Béroudiaux et al. [20] for modeling high-pressure hydrogen–air combustion. Chatzopoulos and Rigopoulos [21] extracted data from non-premixed flamelets at varying strain rates for RANS-PDF simulations of $\text{CH}_4/\text{H}_2/\text{N}_2$ turbulent flames, a low-dimensional manifold sampling methodology further expanded by Franke et al. [22], Ding et al. [15], and Readshaw et al. [23]. Such approaches have also been explored to create initial databases for other storage and retrieval methods by Newale et al. [24]. They demonstrated that both flamelets and partially stirred reactor (PaSR) simulations can effectively generate representative thermochemical states encountered in combustion simulations. The core idea behind these generic canonical problem sampling methods is that, under the same initial working conditions, ensembles of thermochemical states throughout the evolution of chemical systems form a continuous manifold [25].

Despite recent progress, the data preparation process for DNN-based chemical kinetics remains a non-trivial challenge. Constructing large, high-quality datasets that accurately capture the complex thermochemical states encountered in reactive flows is critical yet difficult, particularly for fuels with intricate chemical behavior. Notably, most existing studies in this area have concentrated on hydrocarbon fuels with relatively simplified mechanisms.

92 In contrast, ammonia combustion introduces additional complexity due to
93 nitrogen-bearing species and a wide spectrum of chemical time scales, which
94 significantly complicate both data generation and model learning. To date,
95 limited efforts have been made to extend DNN-based surrogate models to
96 ammonia-fueled systems.

97 To address these gaps, this study explores deep learning-based chem-
98 ical kinetics modeling for NH₃/CH₄ combustion using the comprehensive
99 mechanism by Okafor et al. [26], comprising 59 species and 356 elementary
100 reactions. Thermochemical training data are generated from canonical one-
101 dimensional premixed laminar flames, and a physics-aware data augmenta-
102 tion strategy is introduced to improve coverage in underrepresented regions,
103 particularly near steep thermochemical gradients. The trained models are
104 first validated in 1D laminar flames and subsequently evaluated *a posteriori*
105 in a two-dimensional homogeneous isotropic turbulence (HIT) flame con-
106 figuration to assess generalizability and computational performance. This
107 study advances the application of deep neural networks to ammonia-fueled
108 combustion and presents a scalable framework for accelerating high-fidelity
109 simulations involving complex chemical kinetics.

110 **2. Methodology**

111 *2.1. Deep learning for combustion chemistry integration*

112 A chemical system with N species and M reactions can be expressed as:

$$\sum_{\alpha=1}^N \nu'_{\alpha j} \mathcal{M}_\alpha \Rightarrow \sum_{\alpha=1}^N \nu''_{\alpha j} \mathcal{M}_\alpha \quad \text{for } j = 1, \dots, M, \quad (1)$$

113 Here, \mathcal{M}_α denotes species α , while $\nu'_{\alpha j}$ and $\nu''_{\alpha j}$ represent the molar stoichio-
 114 metric coefficients for species α in reaction j . The reaction rate of species α
 115 is described by the following ODE:

$$\frac{dY_\alpha}{dt} = W_\alpha \sum_{j=1}^M (\nu'_{\alpha j} - \nu''_{\alpha j}) \left\{ K_{fj} \prod_{\alpha=1}^N \left(\frac{\rho Y_\alpha}{W_\alpha} \right)^{\nu'_{\alpha j}} - K_{rj} \prod_{\alpha=1}^N \left(\frac{\rho Y_\alpha}{W_\alpha} \right)^{\nu''_{\alpha j}} \right\} \quad (2)$$

116 where Y_α is the mass fraction and W_α is the molecular weight of species α .
 117 The mixture mass density is represented by ρ , while K_{fj} and K_{rj} are the
 118 forward and reverse rate constants for reaction j . These rate constants are
 119 typically parameterized by temperature T according to Arrhenius models
 120 and also pressure p for pressure-dependent reaction rates.

121 For simulation methods that require real-time computation of the chem-
 122 ical source term in every grid cell and time step, the source terms $\dot{\omega}_\alpha$ are ob-
 123 tained through time integration of the ODE system mentioned above. This
 124 process could be replaced by DNN surrogate models that fit the nonlinear
 125 mapping functions between input-output pairs.

126 As shown in Equation 2, in combustion processes characterized by in-
 127 compressible or weakly compressible flows, the instantaneous reaction source
 128 terms $\dot{\omega}_\alpha$ can be expressed as a function of T , p and the mass fraction vector
 129 $\mathbf{Y} = (Y_1, Y_2, \dots, Y_N)$. Therefore, the input chosen for the neural networks
 130 are local thermochemical parameters $\{T(t), p(t), \mathbf{Y}(t)\}$, and the outputs are
 131 $\{\mathbf{Y}(t + \Delta t) - \mathbf{Y}(t)\}$, which are further used to calculate chemical source
 132 terms provided for the governing PDEs of the reacting flow systems. Figure
 133 1 illustrates the training process of DNN models and their integration with

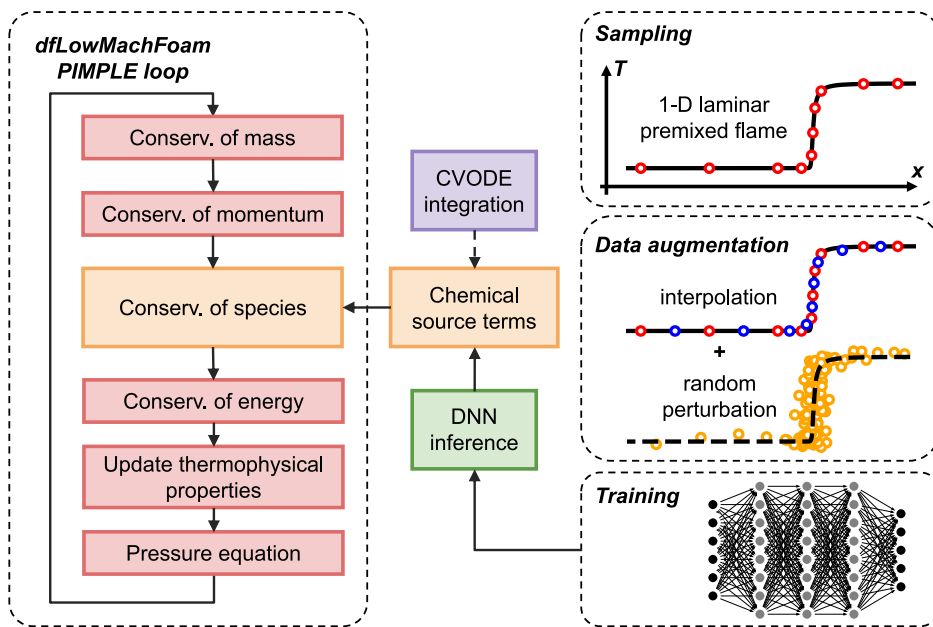


Figure 1: Overview of the training procedure and flow chart for the dfLowMachFoam solver, illustrating the integration of DNN models to provide chemical source terms.

134 reacting flow solvers. The training process starts with the collection of input
135 datasets, which are then fed into the DNN architecture consisting of an input
136 layer, multiple hidden layers, and an output layer. Throughout the training
137 phase, the DNN develops the ability to accurately map input parameters to
138 desired outputs. This is achieved through the optimization of a loss function
139 that measures the difference between the predicted outputs and the actual
140 results generated by the CVODE integrators from SUNDIALS, as provided
141 by Cantera [27].

142 Once trained, the DNN is coupled with the dfLowMachFoam solver from
143 the open-source reacting flow simulation platform DeepFlame [28]. This
144 solver computes the flow field and local conditions of the reacting mixture.
145 At each time step, dfLowMachFoam retrieves the current simulation values
146 and inputs them into the DNN for inference. The DNN then predicts reac-
147 tion rates, which are incorporated into the conservation equations of species.
148 Further details can be found in previous works [29].

149 *2.2. Thermochemical base state collection*

150 Data-driven models, particularly DNNs, heavily depend on the quality of
151 their training data and often struggle with unseen data due to their limited
152 extrapolation capabilities. For DNN models applied to realistic numerical
153 combustion simulations, it is crucial that the training dataset adequately
154 spans the relevant composition space encountered in real-time applications
155 to ensure robustness and applicability.

156 To construct a representative training dataset for premixed combustion
157 simulations, thermochemical base states are derived from lower-dimensional
158 canonical flames, specifically one-dimensional freely propagating premixed

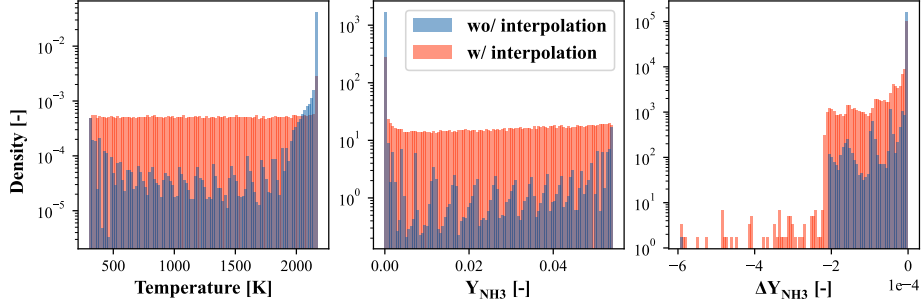


Figure 2: Density distribution of temperature, ammonia mass fraction Y_{NH_3} , and deviations in ammonia concentration ΔY_{NH_3} for datasets with and without interpolation augmentation.

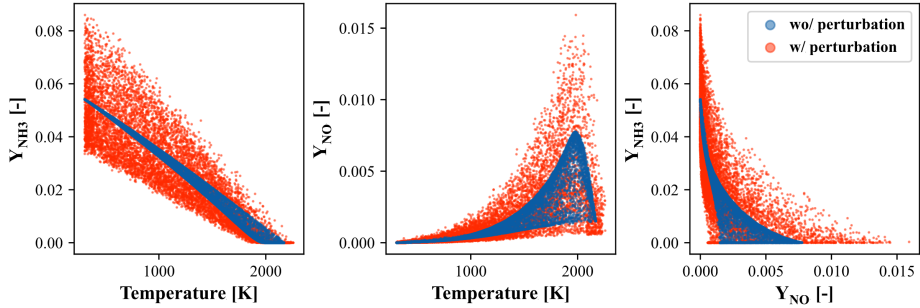


Figure 3: Scatter plots of ammonia mass fraction Y_{NH_3} , nitric oxide mass fraction Y_{NO} against temperature for datasets with and without perturbation augmentation.

159 laminar flames. These base states closely resemble realistic turbulent flames
 160 with similar fuel and oxidizer compositions, making them an ideal starting
 161 point for the training data preparation process.

162 In this study, we focus on DNN models for a specific NH_3 blending ratio
 163 of 60% and stoichiometric equivalence ratio for NH_3/CH_4 mixtures. These
 164 models prove to be able to effectively simulate NH_3/CH_4 premixed flames
 165 with such an NH_3 blending ratio and equivalence ratio under varying turbu-

166 lent flow conditions. This choice keeps the data preparation process in the
167 simplest form, which allows for a more manageable complexity and faster
168 training times. The data preparation process can be easily adjusted for dif-
169 ferent blending and equivalence ratios as needed.

170 The selection of a 60% NH₃ blending ratio is informed by empirical re-
171 sults, which indicate that models trained at this ratio exhibit reduced per-
172 formance compared to those trained at lower blending ratios. This decline
173 in performance is likely due to the larger thermochemical composition space
174 associated with the differing reactivity between ammonia and methane at
175 higher blending ratios. Consequently, focusing on a 60% blending ratio al-
176 lows us to streamline the training process while enhancing model reliability,
177 establishing a solid foundation for future research into more complex config-
178 urations.

179 Although a broader range of blending and equivalence ratios could im-
180 prove the models' applicability, doing so would necessitate larger datasets
181 and more complex architectures, which might compromise computational ef-
182 ficiency. Thus, this focused approach ensures that we maintain a balance
183 between model performance and practical applicability to real-world scenar-
184 ios, ultimately facilitating future advancements in this area of research.

185 To develop a DNN model applicable to turbulent premixed combustion
186 simulations of NH₃/CH₄ mixtures with a NH₃ blending ratio of 60% and a
187 global equivalence ratio of 1, we sample from a single 1D freely propagating
188 premixed laminar flame. The unburnt gas temperature is set to be 300 K,
189 and the ambient pressure is 1 atm. The computational domain consists
190 of premixed fuel/air mixtures in one half and equilibrium states computed

191 using Cantera in the other half. The mesh resolution is designed to resolve the
192 flame thickness with 10 grid cells, totaling 500 cells in the simulation domain.
193 The inlet velocity is determined by the laminar flame speed obtained from
194 Cantera to sustain the flame front within the domain.

195 Simulations are conducted with a fixed time step of $\Delta t = 1e^{-6}$ s for a
196 duration of 2.5 ms with every time step sampled, resulting in an initial
197 dataset of 1,250,000 states. Without the need to sample from multiple
198 lower-dimensional simulations, the training data generation process becomes
199 straightforward and efficient. The reduced complexity in data generation
200 saves time and computational resources, allowing for quicker iterations in
201 model training and easier expansion of the dataset. Additionally, the dataset
202 is easier to manage, which streamlines the workflow and reduces potential
203 errors.

204 *2.3. Data augmentation*

205 Similarly to the findings of Saito et al. [30] and Chen et al. [31], the initial
206 dataset exhibits a higher density of data at lower reaction rates. This issue
207 of data imbalance could potentially result in suboptimal model performance
208 under certain conditions. While various techniques such as density-weighted
209 sampling [30] and data clustering [32, 33, 31] can help mitigate this issue, we
210 present a data augmentation procedure through interpolation based on phys-
211 ical understanding of 1D laminar flame structure. Unlike density-weighted
212 sampling methods, which filter out data and may exclude rare or extreme
213 conditions, our approach adds new data points without necessitating multiple
214 DNNs to learn from clustered data.

215 To ensure that adequate thermochemical states at higher reaction rates

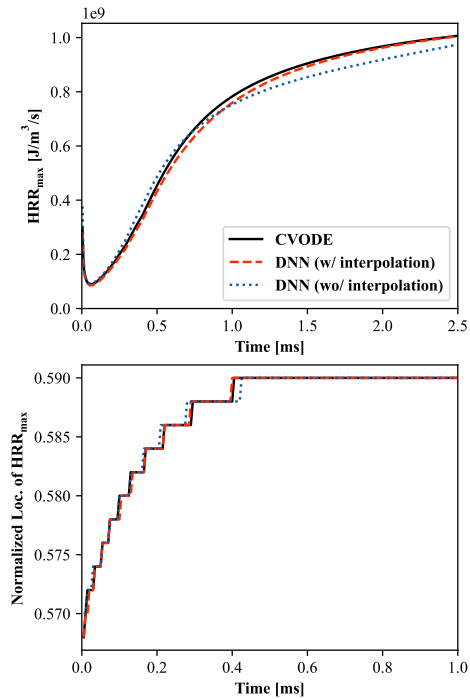


Figure 4: Temporal recordings of the maximum heat release rate (HRR) and the location of the grid cell with the maximum heat release rate, normalized by the simulation domain length.

are included, it is essential to sample more data points from the flame front area. In the case of 1D laminar flames, this region displays significant temperature gradients. Therefore, linear interpolation of other thermochemical properties could be performed based on temperature values to generate additional data points representative of thermochemical conditions within the flame front. For each time step, the 500 thermochemical states are sorted according to temperature, and new states are generated through one-dimensional piecewise linear interpolation of discrete data points (T_{init}, f_{init}), where T_{init} represents the sorted temperatures and f_{init} is either pressure p or mass fraction Y_α . The interpolation is evaluated at points with uniform intervals $\{T_{new}\}$.

Figure 2 illustrates the density distribution of temperature, ammonia mass fraction Y_{NH_3} and ΔY_{NH_3} for one dataset with interpolation augmentation and one without. The dataset with interpolation shows a more uniform distribution for all three parameters. The interpolation process balances sampling frequency across different input parameters and improves the training dataset by alleviating data imbalance. This can enable DNN models to generalize better across input ranges, particularly in regions where data points were previously sparse.

Another issue is that the thermochemical states derived from lower-dimensional flames may not fully capture the relevant composition space required for turbulent combustion simulations. They also follow well-defined trajectories within the sample space, making the trained model susceptible to perturbations or deviations from this manifold. To enhance model robustness, data augmentation through random perturbations can simulate multi-dimensional

241 transport and turbulence effects on the thermochemical structure of the
242 flame, thereby achieving broader coverage of the composition space [15]. In
243 this approach, the original data are discarded in favor of the randomly per-
244 turbed data for training, enabling the DNN to learn from points beyond the
245 lower-dimensional flames and improving its applicability to new states.

246 Both the initial and interpolation-generated states go through random
247 perturbation:

$$T' = T + 100 \cdot X \quad (3)$$

$$p' = p + (\max(p) - \min(p)) \cdot 0.15 \cdot X \quad (4)$$

$$Y'_\alpha = Y_\alpha^{1+0.15 \cdot X} \quad (5)$$

248 where T' , p' , Y'_α represent the perturbed values, and X is a random number
249 uniformly distributed between -1 and 1. Figure 3 shows the composition
250 space spanned by datasets with and without perturbation augmentation. It
251 is evident that the coverage of the composition space is effectively broad-
252 ened through random perturbation. However, if left unconstrained, it may
253 produce numerous nonphysical states, which can adversely affect model ac-
254 curacy in critical regions. Such nonphysical states are primarily observed
255 in areas with higher initial temperatures, corresponding to near-equilibrium
256 states, and demonstrate negative heat release rates of significant magnitude.
257 The perturbation procedure is performed for several rounds, collecting the
258 perturbed data at each iteration. After filtering out the nonphysical states,
259 approximately 8,000,000 valid perturbed states are randomly chosen as the
260 final training dataset.

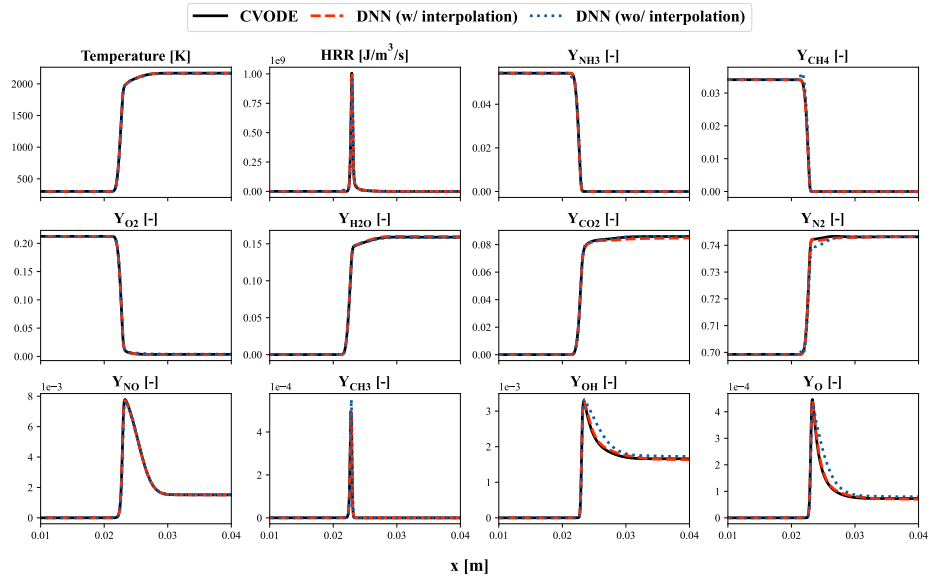


Figure 5: Temperature, heat release rate (HRR), and species mass fractions profiles in physical space obtained at 2.5 ms in 1D laminar premixed flame simulations using DNN inference or CVODE integration for chemical source terms.

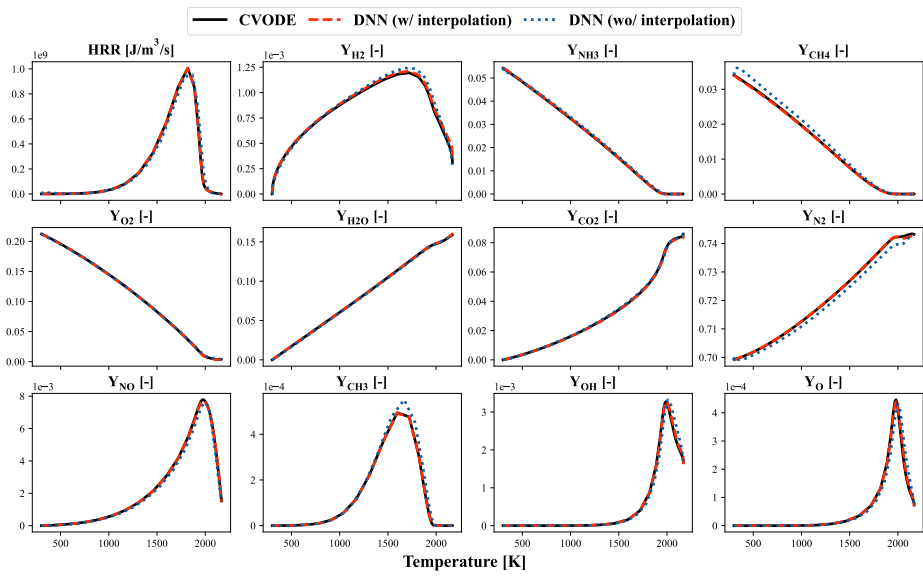


Figure 6: Heat release rate (HRR), and species mass fractions profiles in temperature space obtained at 2.5 ms in 1D laminar premixed flame simulations using DNN inference or CVODE integration for chemical source terms.

261 2.4. Model architecture and training

262 The DNN model utilized is a multilayer perceptron (MLP) architecture,
263 comprising an input layer, an output layer, and four hidden layers, each
264 containing 800 neurons. The mass fraction of the inert species argon is ex-
265 cluded from the model output, as it remains constant throughout the reaction
266 process and does not require modeling. The species mass fractions are trans-
267 formed using the Box-Cox transformation to map data of all magnitudes to
268 a similar scale:

$$\text{BCT}(x) = \frac{x^\lambda - 1}{\lambda} \quad \text{where } \lambda = 0.1 \quad (6)$$

269 The Box-Cox transformation maps the species mass fractions within the
270 range [0, 1] to [-10, 0]. This mapping reduces the non-linearity of the data,
271 which may exhibit very small scales, and provides a more uniform data distri-
272 bution. The output mass fractions are set as $\{\text{BCT}(\mathbf{Y}(t+\Delta t)) - \text{BCT}(\mathbf{Y}(t))\}$.
273 Both the input and output data are normalized using Z-score normalization.
274 Other aspects of the training procedure are consistent with previous studies
275 [29].

276 2.5. Premixed flame in two-dimensional homogeneous isotropic turbulence

277 To validate the DNN models in combustion simulations, simulations of
278 a flame kernel ignition of premixed NH₃/CH₄ mixture in two-dimensional
279 homogeneous isotropic turbulence (HIT) were conducted. Similar setups
280 have been used in previous works [29, 34].

281 In the simulation, a square computational domain of $L \times L = 28 \times 28 \text{ mm}^2$
282 is used, initialized with a premixed stoichiometric mixture of 60%NH₃/40%CH₄
283 at 300 K and 1 atm. To ignite the mixture, a circular hot spot with a ra-
284 dius of $L/10$ filled with equilibrium state gases is placed in the center of

285 the domain. The HIT generation approach in [35] is adopted and the fully
286 evolved velocity field is then mapped to the computational domain as the ini-
287 tial flow field. Boundary conditions are set to zero gradient for temperature
288 and species mass fractions, and a non-reflective wave transmissive condition
289 is used for pressure and velocity. The domain is uniformly discretized with
290 512×512 grids to ensure sufficient resolution for both flame and turbulence.

291 3. Results

292 3.1. Application to 1D freely propagating premixed laminar flame

293 The DNN models are first tested in the 1D freely propagating premixed
294 laminar flame used for training data generation. We compare the results
295 from DNN models trained on datasets with and without interpolation aug-
296 mentation against simulations using CVODE for chemistry integration.

297 In Figure 4, the upper panel displays the trajectory of the maximum
298 heat release rate during the simulations. The DNN trained on the dataset
299 with interpolation closely follows the CVODE results, indicating improved
300 accuracy compared to the DNN trained on the dataset without interpolation,
301 which under-predicted reaction intensity. The lower panel illustrates the
302 location of the maximum heat release rate, highlighting flame propagation.
303 Here, the DNN without interpolation exhibits more fluctuating behavior,
304 while the DNN trained with interpolation provides a more stable and accurate
305 prediction of flame location. This improved performance suggests that the
306 DNN trained on the dataset with interpolation is more adept at capturing the
307 dynamics of reactive states. The inaccuracies observed in the DNN without
308 interpolation could lead to significant errors in predicting flame propagation

309 behavior.

310 Figure 5 and 6 show the flame structure obtained at 2.5 ms for CVODE
311 and the two DNN models. The results from the DNN models trained on
312 the dataset without interpolation reveal discrepancies in the NH₃ and CH₄
313 profiles on the unburnt side of the flame, as well as in the profiles of interme-
314 diate species like OH and O behind the flame front. These discrepancies are
315 particularly evident in the progress variable space, where a shift in species
316 profiles occurs for the DNN without interpolation. In contrast, the DNN
317 trained on data with interpolation demonstrates better alignment with the
318 CVODE results, indicating superior predictive capability.

319 *3.2. Application to premixed flame in two-dimensional homogeneous isotropic*
320 *turbulence*

321 The DNN trained on data with interpolation is adopted for the 2D case.
322 We compare the results from DNN inference against simulations using CVODE
323 for chemistry integration. Both simulations are conducted for 4 ms, during
324 which the flame kernel propagates near the boundary. The simulation is
325 then stopped to prevent boundary conditions from producing nonphysical
326 behavior.

327 Figure 7 illustrates the trajectory of maximum temperature and maxi-
328 mum heat release rate during the simulations. The results from the DNN
329 align well with those obtained from the CVODE simulations for both met-
330 rics, with a maximum difference of approximately 5 K in the maximum
331 temperature. This close agreement demonstrates the DNN’s capability to
332 accurately capture the key dynamics of the combustion process. However, it
333 also indicates that there is still room for improvement in prediction accuracy

334 for equilibrium states, despite the model’s effectiveness in predicting rapidly
335 changing conditions across the flame front.

336 Several factors may contribute to this behavior. First, the lack of atomic
337 conservation in DNN predictions can lead to discrepancies. Béroudiaux et
338 al. reported that DNNs can diverge when predicting equilibrium states, and
339 that incorporating atomic conservation corrections can effectively address
340 this issue [20]. Although some studies [19, 36] have discussed correction pro-
341 cedures, Béroudiaux et al. [20] emphasized that post-inference corrections do
342 not always yield improved results. It may be more advantageous to integrate
343 atomic conservation directly into the model architecture as hard constraints,
344 as suggested by Rohrhofer et al. in [37].

345 Another potential reason for the decreased model performance in equi-
346 librium states is the multi-scale nature of combustion chemical kinetics.
347 Rohrhofer et al. [37] et al. highlighted that using loss functions based on
348 absolute errors can result in smaller scale changes being learned less accu-
349 rately. While the data transformation using Box-Cox transformation in this
350 study may alleviate some multi-scale issues, accuracy problems related to the
351 absolute loss function are likely to persist.

352 Figure 8 presents calculations of flame area in 2D HIT flame simulations,
353 providing a general description of flame kernel development. The results indi-
354 cate that the DNN predictions align well with the CVODE results regarding
355 flame area. This reaffirms that the DNN models used in this study possess
356 sufficient accuracy for predicting reacting states, resulting in good agreement
357 with numerical integration methods when capturing flame dynamics.

358 Figure 9, 10, and 11 show scalar fields of temperature, heat release rate,

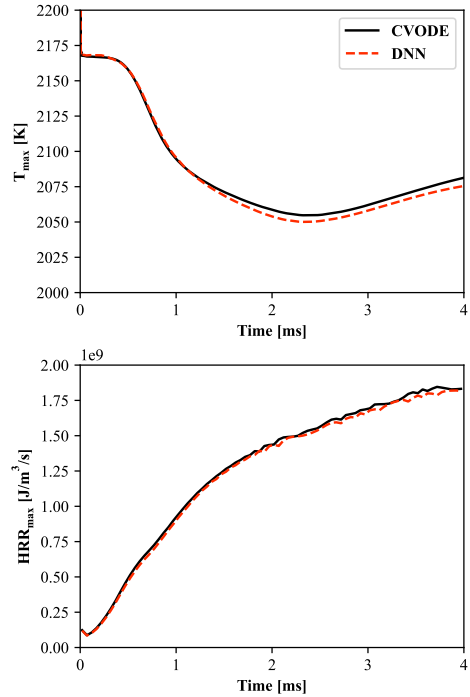


Figure 7: Temporal recordings of the maximum temperature and maximum heat release rate (HRR) in 2D HIT flame simulation.

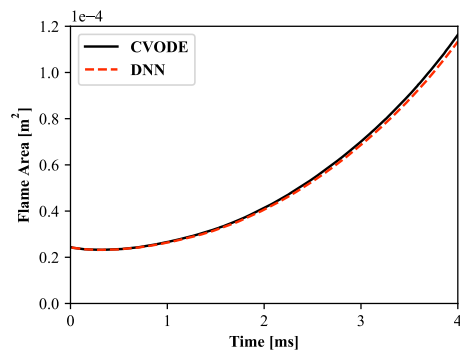


Figure 8: Calculations of flame area in 2D HIT flame simulations.

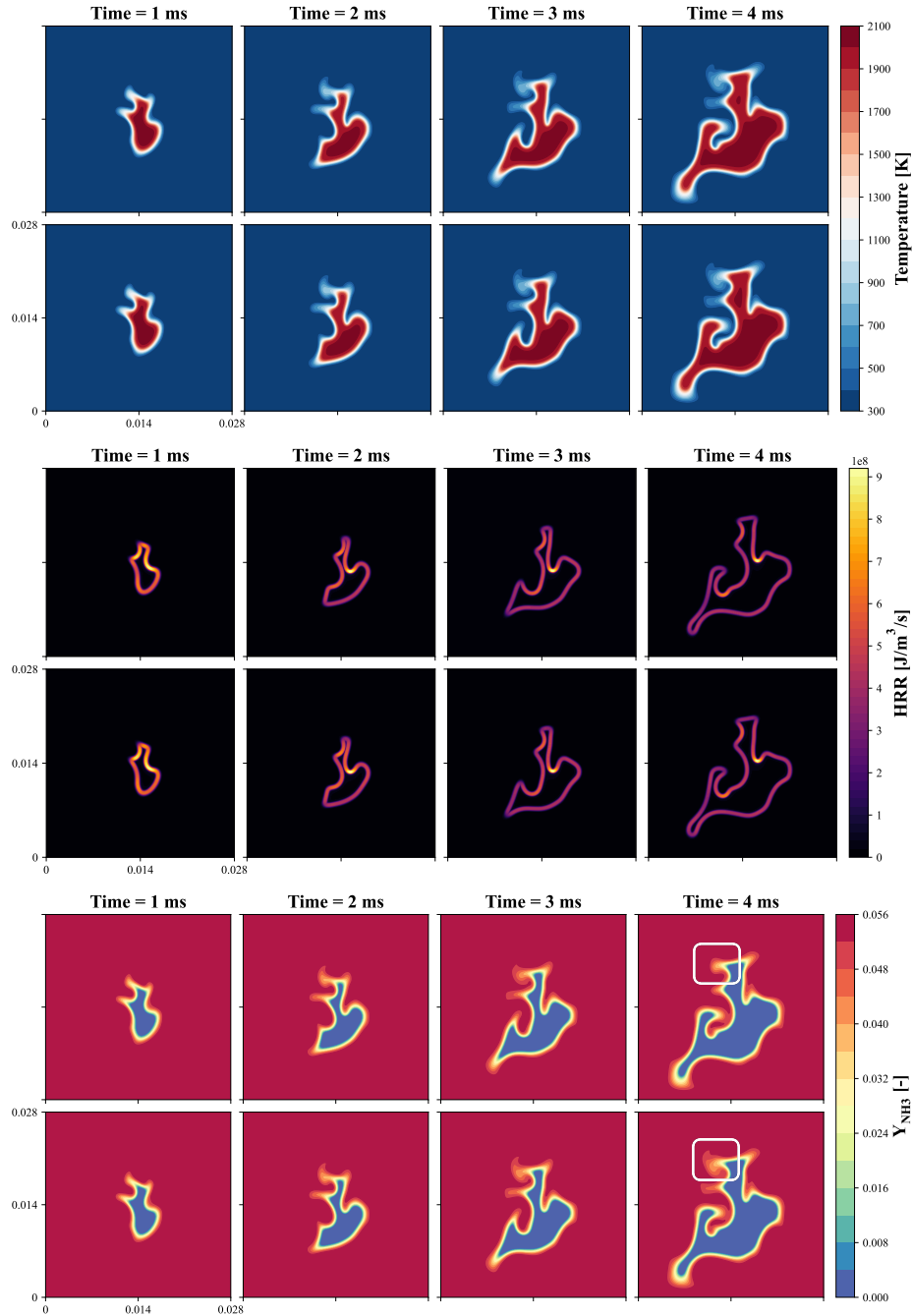


Figure 9: 2D simulations - scalar fields of temperature, heat release rate (HRR), and species mass fractions for NH_3 (Y_{NH_3}) obtained through DNN (top) and CVODE (bottom).

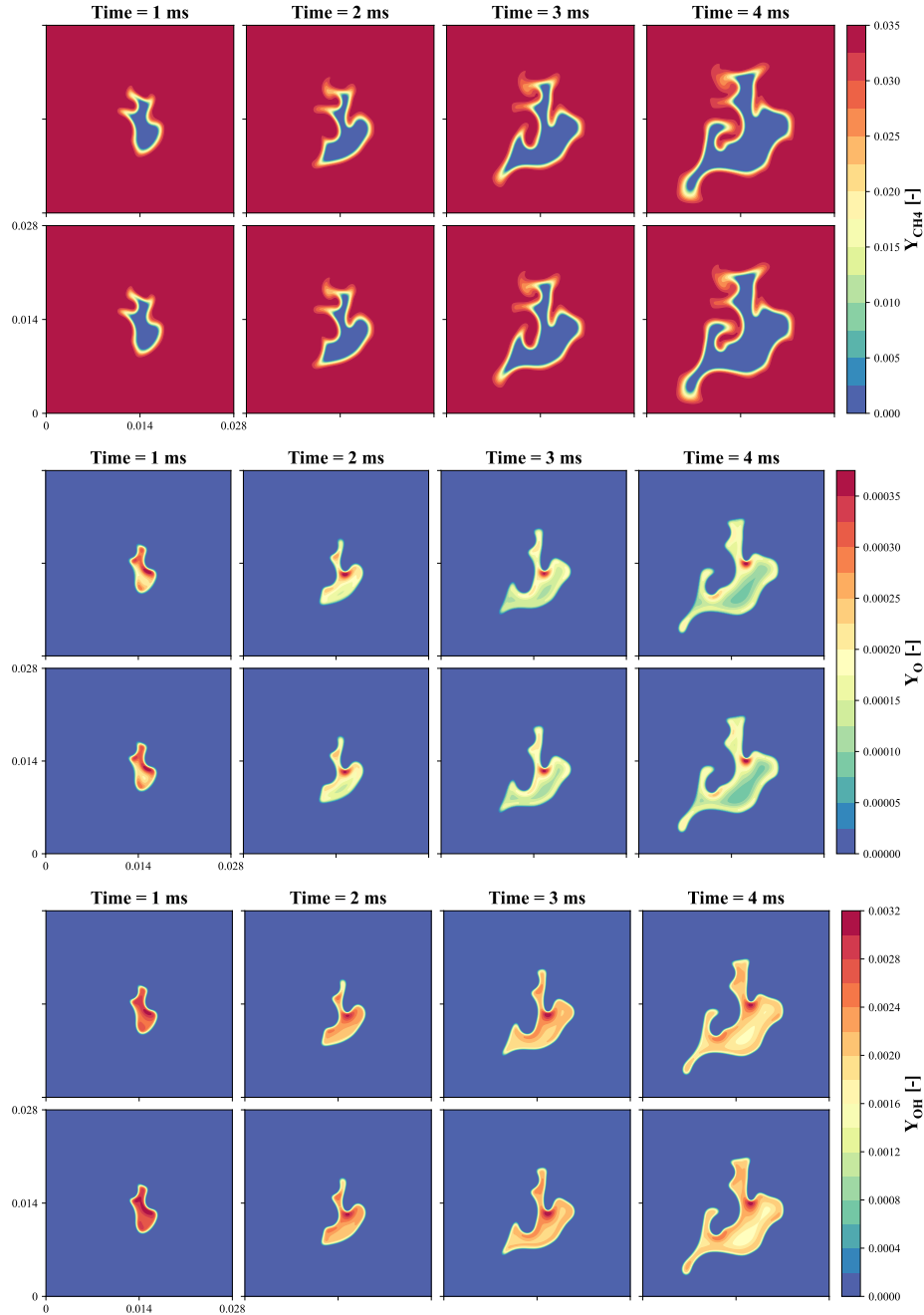


Figure 10: 2D simulations - scalar fields of species mass fractions for CH_4 (Y_{CH_4}), O (Y_{O}), and OH (Y_{OH}) obtained through DNN (top) and CVODE (bottom).

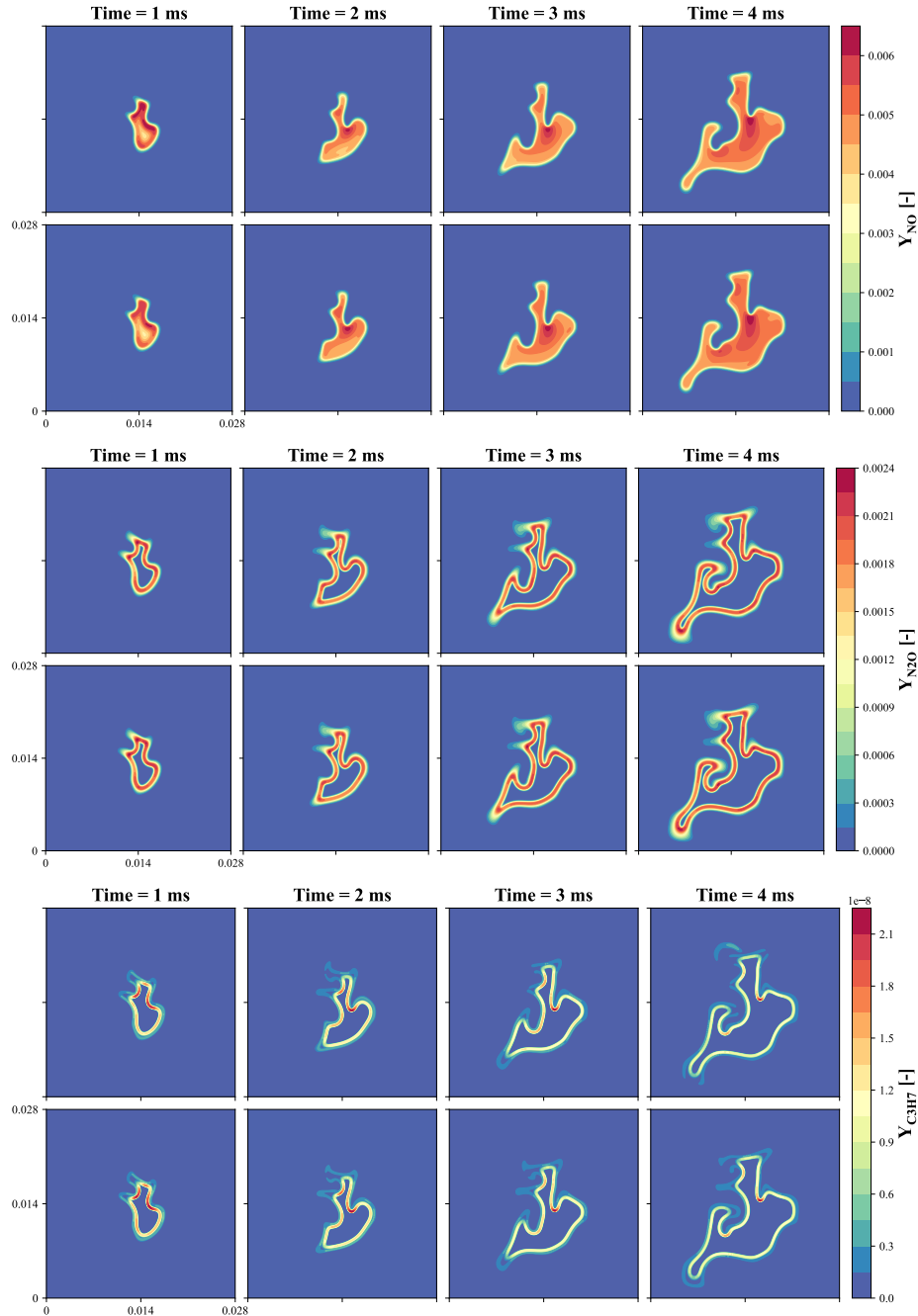


Figure 11: 2D simulations - scalar fields of species mass fractions for NO (Y_{NO}), N₂O (Y_{N_2O}), and C₃H₇ ($Y_{C_3H_7}$) obtained through DNN (top) and CVODE (bottom).

and species mass fractions obtained through DNN and CVODE simulations. The results demonstrate good overall agreement between the DNN and CVODE simulations, indicating that DNN simulations effectively capture the spatial distributions of these quantities throughout iterative model inference and flow field property updates.

Small discrepancies are observed in Y_{NH_3} profiles, particularly in the top left corner of the flame at 4 ms. When interpreted in conjunction with the scalar fields of temperature and the mass fractions of other minor species, such as OH, NO, and N₂O, it becomes evident that the thermochemical composition of this region is predominantly influenced by convection rather than by reaction. This leads to a higher temperature compared to unburnt gases, despite a low heat release rate. Such compositions present challenges for DNN prediction due to the small-scale changes in species composition, similar to the issues encountered in equilibrium states.

Additionally, the differing reactivity between NH₃ and CH₄ may expand the possible composition space, highlighting the need for further exploration of these dynamics to enhance model accuracy and predictive capabilities. Figure 11 presents scalar fields of $Y_{\text{C}_3\text{H}_7}$, demonstrating that, at later time steps, discrepancies in $Y_{\text{C}_3\text{H}_7}$ become larger. CVODE results indicate both production and consumption of C₃H₇ on the unburnt side of the flame, while DNN simulations fail to capture this behavior accurately.

A similar phenomenon is observed in the 1D laminar premixed flame simulation using Cantera, as indicated by the small secondary peak of $Y_{\text{C}_3\text{H}_7}$ in Figure 12. To accurately capture such dynamics, it is essential to include related thermochemical compositions in the training data and ensure they are

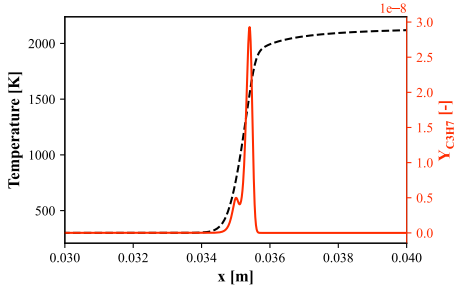


Figure 12: Temperature and C_3H_7 mass fraction profiles from 1D freely propagating pre-mixed laminar flame simulated using Cantera.

384 learned effectively. This underscores the importance of prior knowledge about
 385 the chemical kinetic system when developing DNN surrogates for chemistry
 386 integration. However, since the species C_3H_7 was not included in the sen-
 387 sitivity analysis during mechanism development [26], and considering that
 388 important radicals such as O and OH, as well as emission products like NO
 389 and N_2O are simulated correctly, the discrepancies in $Y_{C_3H_7}$ can be regarded
 390 as acceptable.

391 The simulations were conducted using 32 Intel Xeon Gold 6330 CPU
 392 cores, with an additional 2 NVIDIA GeForce RTX 4090 GPUs used for DNN
 393 inference. Compared to previous works [29], data transfer between CPU and
 394 GPU has been optimized through data batching, which simplified the process
 395 of invoking PyTorch for DNN inference and improved data transfer speed as
 396 well as memory consumption, allowing the solver to perform better when
 397 processing large-scale data. As a result, DNN simulations achieved a 526
 398 times speedup in chemistry source term calculations. When considering the
 399 overall calculation, this translates to a total speedup of 20 times compared
 400 to the simulation using CVODE.

401 **4. Conclusions**

402 In this work, DNN models were developed as surrogate models for chem-
403 istry integration in premixed NH₃/CH₄ combustion simulations. Training
404 data were generated through simulations of a 1D laminar premixed flame,
405 with data augmentation techniques employed to enhance the dataset. Inter-
406 polation was used to increase the number of reacting states, while random
407 perturbation was applied to simulate the effects of turbulence and transport
408 on the thermochemical structure of the flame. These models are intended
409 for application to premixed NH₃/CH₄ combustion under varying flow condi-
410 tions, given that the blending ratio and equivalence ratio are the same as the
411 sampled 1D laminar flame.

412 DNN models trained on datasets with and without interpolation augmen-
413 tation were tested in 1D laminar flame simulations and compared to results
414 obtained using direct integration through CVODE. The DNN model trained
415 on the interpolated dataset demonstrated superior performance, highlighting
416 the effectiveness of maintaining a balanced training dataset.

417 In 2D HIT flame simulations, the DNN models achieved an 526 times
418 speedup in chemistry-related calculations, resulting in a total speedup of 20
419 times compared to CVODE simulations. The DNN predictions for maximum
420 heat release rate and flame area closely aligned with CVODE results. Scalar
421 fields for temperature, heat release rate, and species mass fractions showed
422 good overall agreement, affirming the reliability of the DNN integrator in
423 turbulent combustion simulations.

424 Limitations of the DNN model in this study are also acknowledged. En-
425 hancements are needed to accurately predict minor species and equilibrium

⁴²⁶ states, with a significant area for improvement being the inclusion of related
⁴²⁷ thermochemical compositions in the training data. Future work will focus on
⁴²⁸ addressing these limitations and further refining the DNN models to enhance
⁴²⁹ their predictive capabilities in complex combustion scenarios.

References

- [1] Valera-Medina A, Xiao H, Owen-Jones M, David W, Bowen P. Ammonia for power. *Prog in Energy and Combust Sci.* 2018;69:63–102.
<https://doi.org/10.1016/j.pecs.2018.07.001>.
- [2] Valera-Medina A, Amer-Hatem F, Azad A, Dedoussi I, De Joannon M, Fernandes R, et al. Review on Ammonia as a Potential Fuel: From Synthesis to Economics. *Energy & Fuels.* 2021;35(9):6964–7029.
<https://doi.org/10.1021/acs.energyfuels.0c03685>.
- [3] Kojima Y, Yamaguchi M. Ammonia as a hydrogen energy carrier. *Int J of Hydrog Energy.* 2022;47(54):22832–22839.
<https://doi.org/10.1016/j.ijhydene.2022.05.096>.
- [4] Dimitriou P, Javaid R. A review of ammonia as a compression ignition engine fuel. *Int J of Hydrog Energy.* 2020;45(11):7098–7118.
<https://doi.org/10.1016/j.ijhydene.2019.12.209>.
- [5] Yapicioglu A, Dincer I. A review on clean ammonia as a potential fuel for power generators. *Renew and Sustain Energy Rev.* 2019;103:96–108.
<https://doi.org/10.1016/j.rser.2018.12.023>.

- [6] Aziz M, Wijayanta A, Nandiyanto A. Ammonia as Effective Hydrogen Storage: A Review on Production, Storage and Utilization. *Energies.* 2020;13(12):3062. <https://doi.org/10.3390/en13123062>.
- [7] Chai W, Bao Y, Jin P, Tang G, Zhou L. A review on ammonia, ammonia-hydrogen and ammonia-methane fuels. *Renew and Sustain Energy Rev.* 2021;147:111254. <https://doi.org/10.1016/j.rser.2021.111254>.
- [8] Lu T, Law C. Toward accommodating realistic fuel chemistry in large-scale computations. *Prog in Energy and Combust Sci.* 2009;35(2):192–215. <https://doi.org/10.1016/j.pecs.2008.10.002>.
- [9] Mikulčić H, Baleta J, Wang X, Wang J, Qi F, Wang F. Numerical simulation of ammonia/methane/air combustion using reduced chemical kinetics models. *Int J of Hydrom Energy.* 2021;46(45):23548–23563. <https://doi.org/10.1016/j.ijhydene.2021.01.109>.
- [10] Meuwly M. Machine Learning for Chemical Reactions. *Chem Rev.* 2021;121(16):10218–10239. <https://doi.org/10.1021/acs.chemrev.1c00033>.
- [11] Zhang T, Yi Y, Xu Y, Chen Z, Zhang Y, E W, et al. A multi-scale sampling method for accurate and robust deep neural network to predict combustion chemical kinetics. *Combust and Flame.* 2022;245:112319. <https://doi.org/10.1016/j.combustflame.2022.112319>.
- [12] Echekki T, Farooq A, Ihme M, Sarathy S. Machine learning for combustion chemistry. In: Machine learning and its application to reacting

flows: ML and combustion. Springer International Publishing Cham; 2023, p. 117–147.

- [13] Ihme M, Chung W. Artificial intelligence as a catalyst for combustion science and engineering. *Proc of the Combust Inst.* 2024;40(1-4):105730. <https://doi.org/10.1016/j.proci.2024.105730>.
- [14] Ren Z, Lu Z, Hou L, Lu L. Numerical simulation of turbulent combustion: Scientific challenges. *Sci China Phys, Mech & Astron.* 2014;57(8):1495–1503. <https://doi.org/10.1007/s11433-014-5507-0>.
- [15] Ding T, Readshaw T, Rigopoulos S, Jones W. Machine learning tabulation of thermochemistry in turbulent combustion: An approach based on hybrid flamelet/random data and multiple multilayer perceptrons. *Combust and Flame.* 2021;231:111493. <https://doi.org/10.1016/j.combustflame.2021.111493>.
- [16] Nikolaou Z, Vervisch L, Domingo P. Criteria to switch from tabulation to neural networks in computational combustion. *Combust and Flame.* 2022;246:112425. <https://doi.org/10.1016/j.combustflame.2022.112425>.
- [17] An J, He G, Luo K, Qin F, Liu B. Artificial neural network based chemical mechanisms for computationally efficient modeling of hydrogen/carbon monoxide/kerosene combustion. *Int J of Hydrog Energy.* 2020;45(53):29594–29605. <https://doi.org/10.1016/j.ijhydene.2020.08.081>.
- [18] Chi C, Janiga G, Thévenin D. On-the-fly artificial neural network for chemical kinetics in direct numerical simulations of

- premixed combustion. *Combust and Flame.* 2021;226:467–477.
<https://doi.org/10.1016/j.combustflame.2020.12.038>.
- [19] Wan K, Barnaud C, Vervisch L, Domingo P. Chemistry reduction using machine learning trained from non-premixed micro-mixing modeling: Application to DNS of a syngas turbulent oxy-flame with side-wall effects. *Combust and Flame.* 2020;220:119–129.
<https://doi.org/10.1016/j.combustflame.2020.06.008>.
- [20] Béroudiaux A, Vervisch L, Domingo P. Artificial neural network chemistry solving for high-pressure hydrogen-air combustion. *Int J of Hydrog Energy.* 2025;109:669–683.
<https://doi.org/10.1016/j.ijhydene.2025.02.054>.
- [21] Chatzopoulos A, Rigopoulos S. A chemistry tabulation approach via Rate-Controlled Constrained Equilibrium (RCCE) and Artificial Neural Networks (ANNs), with application to turbulent non-premixed CH₄/H₂/N₂ flames. *Proc of the Combust Inst.* 2013;34(1):1465–1473.
<https://doi.org/10.1016/j.proci.2012.06.057>.
- [22] Franke L, Chatzopoulos A, Rigopoulos S. Tabulation of combustion chemistry via Artificial Neural Networks (ANNs): Methodology and application to LES-PDF simulation of Sydney flame L. *Combust and Flame.* 2017;185:245–260.
<https://doi.org/10.1016/j.combustflame.2017.07.014>.
- [23] Readshaw T, Franke L, Jones W, Rigopoulos S. Simulation of turbulent premixed flames with machine learning - tabu-

- lated thermochemistry. *Combust and Flame.* 2023;258:113058. <https://doi.org/10.1016/j.combustflame.2023.113058>.
- [24] Newale A, Sharma P, Pope S, Pepiot P. A feasibility study on the use of low-dimensional simulations for database generation in adaptive chemistry approaches. *Combust Theory and Model.* 2022;26(7):1239–1261. <https://doi.org/10.1080/13647830.2022.2137062>.
- [25] Maas U, Pope S. Simplifying chemical kinetics: Intrinsic low-dimensional manifolds in composition space. *Combust and Flame.* 1992;88(3-4):239–264. [https://doi.org/10.1016/0010-2180\(92\)90034-M](https://doi.org/10.1016/0010-2180(92)90034-M).
- [26] Okafor E, Naito Y, Colson S, Ichikawa A, Kudo T, Hayakawa A, et al. Experimental and numerical study of the laminar burning velocity of CH₄–NH₃–air premixed flames. *Combust and Flame.* 2018;187:185–198. <https://doi.org/10.1016/j.combustflame.2017.09.002>.
- [27] Goodwin D, Moffat H, Schoegl I, Speth R, Weber B. Cantera: An Object-oriented Software Toolkit for Chemical Kinetics, Thermodynamics, and Transport Processes. 2022. <https://doi.org/10.5281/ZENODO.6387882>.
- [28] Mao R, Lin M, Zhang Y, Zhang T, Xu Z, Chen Z. DeepFlame: A deep learning empowered open-source platform for reacting flow simulations. *Comput Phys Commun.* 2023;291:108842. <https://doi.org/10.1016/j.cpc.2023.108842>.
- [29] Li H, Yang R, Xu Y, Zhang M, Mao R, Chen Z. Comprehensive deep learning for combustion chemistry integration: Multi-fuel gener-

- alization and *a posteriori* validation in reacting flow. *Phys of Fluids.* 2025;37(1):015162. <https://doi.org/10.1063/5.0248582>.
- [30] Saito M, Xing J, Nagao J, Kurose R. Data-driven simulation of ammonia combustion using neural ordinary differential equations (NODE). *Appl in Energy and Combust Sci.* 2023;16:100196. <https://doi.org/10.1016/j.jaecs.2023.100196>.
- [31] Chen X, Mehl C, Faney T, Di Meglio F. Clustering-Enhanced Deep Learning Method for Computation of Full Detailed Thermochemical States via Solver-Based Adaptive Sampling. *Energy & Fuels.* 2023;37(18):14222–14239. <https://doi.org/10.1021/acs.energyfuels.3c01955>.
- [32] Blasco J, Fueyo N, Dopazo C, Chen J. A self-organizing-map approach to chemistry representation in combustion applications. *Combust Theory and Model.* 2000;4(1):61–76. <https://doi.org/10.1088/1364-7830/4/1/304>.
- [33] Han X, Jia M, Chang Y, Li Y. An improved approach towards more robust deep learning models for chemical kinetics. *Combust and Flame.* 2022;238:111934. <https://doi.org/10.1016/j.combustflame.2021.111934>.
- [34] Cai Y, Yang R, Li H, Xu J, Xiao K, Chen Z, et al. Efficient machine learning method for supercritical combustion: Predicting real-fluid properties and chemical ODEs. *Aerosp Sci and Technol.* 2025;159:110034. <https://doi.org/10.1016/j.ast.2025.110034>.

- [35] Vuorinen V, Keskinen K. DNSLab: A gateway to turbulent flow simulation in Matlab. *Comput Phys Commun*. 2016;203:278–289. <https://doi.org/10.1016/j.cpc.2016.02.023>.
- [36] Readshaw T, Jones W, Rigopoulos S. On the incorporation of conservation laws in machine learning tabulation of kinetics for reacting flow simulation. *Phys of Fluids*. 2023;35(4):047103. <https://doi.org/10.1063/5.0143894>.
- [37] Rohrhofer F, Posch S, Gößnitzer C, García-Oliver J, Geiger B. Utilizing neural networks to supplant chemical kinetics tabulation through mass conservation and weighting of species depletion. *Energy and AI*. 2024;16:100341. <https://doi.org/10.1016/j.egyai.2024.100341>.